

1-2016

# Near-Barrierless Ammonium Bisulfate Formation via a Loop-Structure Promoted Proton-Transfer Mechanism on the Surface of Water

Lei Li

*University of Nebraska-Lincoln*

Manoj Kumar

*University of Nebraska-Lincoln, chem.manoj@gmail.com*

Chongqin Zhu

*University of Nebraska-Lincoln, czhu5@unl.edu*

Jie Zhong


*University of Nebraska-Lincoln, jzhong4@unl.edu*

Joseph S. Francisco

*University of Nebraska-Lincoln, frjoseph@sas.upenn.edu*

*See next page for additional authors*

Follow this and additional works at: <https://digitalcommons.unl.edu/chemzeng>

 Part of the [Analytical Chemistry Commons](#), [Materials Chemistry Commons](#), and the [Physical Chemistry Commons](#)

---

Li, Lei; Kumar, Manoj; Zhu, Chongqin; Zhong, Jie; Francisco, Joseph S.; and Zeng, Xiao Cheng, "Near-Barrierless Ammonium Bisulfate Formation via a Loop-Structure Promoted Proton-Transfer Mechanism on the Surface of Water" (2016). *Xiao Cheng Zeng Publications*. 150.

<https://digitalcommons.unl.edu/chemzeng/150>

This Article is brought to you for free and open access by the Published Research - Department of Chemistry at DigitalCommons@University of Nebraska - Lincoln. It has been accepted for inclusion in Xiao Cheng Zeng Publications by an authorized administrator of DigitalCommons@University of Nebraska - Lincoln.

---

**Authors**

Lei Li, Manoj Kumar, Chongqin Zhu, Jie Zhong, Joseph S. Francisco, and Xiao Cheng Zeng

# Near-Barrierless Ammonium Bisulfate Formation via a Loop-Structure Promoted Proton-Transfer Mechanism on the Surface of Water

Lei Li,<sup>1</sup> Manoj Kumar,<sup>1</sup> Chongqin Zhu,<sup>1</sup> Jie Zhong,<sup>1</sup>  
Joseph S. Francisco,<sup>1</sup> and Xiao Cheng Zeng<sup>1,2</sup>

<sup>1</sup> Department of Chemistry, University of Nebraska–Lincoln, Lincoln, Nebraska 68588, United States  
<sup>2</sup> Collaborative Innovation Center of Chemistry for Energy Materials, University of Science and Technology of China,  
Hefei, Anhui 230026, China

Corresponding authors — X. C. Zeng, xzeng1@unl.edu ; J. S. Francisco, jfrancisco3@unl.edu

## Abstract

In the atmosphere, a well-known and conventional pathway toward the formation of ammonium sulfate is through the neutralization of sulfuric acid with ammonia ( $\text{NH}_3$ ) in water droplets. Here, we present direct ab initio molecular dynamics simulation evidence of the formation of ammonium bisulfate ( $\text{NH}_4\text{HSO}_4$ ) from the hydrated  $\text{NH}_3$  and  $\text{SO}_3$  molecules in a water trimer as well as on the surface of a water droplet. This reaction suggests a new mechanism for the formation of ammonium sulfate in the atmosphere, especially when the concentration of  $\text{NH}_3$  is high (e.g.,  $\sim 10 \mu\text{g m}^{-3}$ ) in the air. Contrary to the water monomer and dimer, the water trimer enables near-barrierless proton transfer via the formation of a unique loop structure around the reaction center. The formation of the loop structure promotes the splitting of a water molecule in the proton-transfer center, resulting in the generation a  $\text{NH}_4^+/\text{HSO}_4^-$  ion pair. The loop-structure promoted proton-transfer mechanism is expected to be ubiquitous on the surface of cloud droplets with adsorbed  $\text{NH}_3$  and  $\text{SO}_3$  molecules and, thus, may play an important role in the nucleation of aerosol particles (e.g., fine particles  $\text{PM}_{2.5}$ ) in water droplets.

Atmospheric aerosols have become a central topic in the environmental and atmospheric science due to their influence on the biosphere,<sup>1</sup> climate,<sup>2–6</sup> and public health.<sup>7,8</sup> Many experimental studies have shown that sulfate salts (ammonium sulfate in particular) are one of the main constituents in aerosols (e.g., fine particles  $\text{PM}_{2.5}$ ) and play a key role in the formation of sulfur-containing aerosols by acting as condensation nuclei.<sup>9–14</sup> Investigation of the formation mechanism of ammonium sulfates in the atmosphere is both timely and important to the understanding of the nucleation and growth of aerosol particles, thereby may lead to better science-based solutions in resolving the severe haze problems (such as those occurred recently in the winter season of eastern China).

In the atmosphere, ammonium sulfate is generally believed to be formed via the neutralization of sulfuric acid ( $\text{H}_2\text{SO}_4$ ) with ammonia ( $\text{NH}_3$ ) molecules.<sup>15</sup> Although the sulfuric acid formation from the bimolecular reaction between  $\text{SO}_3$  and  $\text{H}_2\text{O}$  entails a

high activation energy barrier (28–32 kcal/mol),<sup>16–18</sup> recent studies have shown that the reaction energetics can be significantly influenced by the participation of four or more water molecules or other atmospheric molecules such as the  $\text{HO}_2$  radical and formic acid.<sup>19,20</sup> In a highly polluted atmosphere, the concentration of  $\text{NH}_3$  may rise up to  $10 \mu\text{g m}^{-3}$  ( $\sim 3.5 \times 10^{17} \cdot \text{m}^{-3}$ ), much higher than that of the  $\text{HO}_2$  radical and formic acid and may even be comparable with that of water monomers ( $\sim 7.73 \times 10^{17}$  molecules  $\cdot \text{m}^{-3}$  at 100 % relative humidity and 298.15 K).<sup>21</sup> This suggests that ammonia molecules can play a more direct role in the formation of ammonium sulfate. An early study has shown that ammonia can act as a catalyst to promote the formation of sulfuric acid by lowering the energy barrier to  $\sim 3.80$  kcal/mol, but without the formation of  $\text{NH}_4^+$ .<sup>22</sup> Another possible mechanism<sup>23</sup> considered involves the barrierless formation of a donor–acceptor  $\text{NH}_3\text{–SO}_3$  complex, which has a binding energy of  $\sim 20$  kcal/mol,<sup>24–27</sup> much higher than that of the  $\text{H}_2\text{O–SO}_3$  complex ( $\sim 7.9$  kcal/mol).<sup>16</sup> Though the  $\text{NH}_3\text{–SO}_3$  complex can also lead to sulfamic acid,<sup>26,28</sup> the reaction is endothermic with a high barrier of  $\sim 16.13$  kcal/mol.<sup>22</sup> Although recent experimental studies have shown the promoting role of  $\text{NH}_3$  in the nucleation of aerosol particles, a detailed chemical mechanism for the formation of ammonium sulfate from  $\text{NH}_3$  and  $\text{SO}_3$  is still largely unknown.

Here, we show direct ab initio molecular dynamics (AIMD) simulation evidence of the near-barrierless formation of ammonium bisulfate ( $\text{NH}_4\text{HSO}_4$ ) from the hydrated  $\text{NH}_3$  and  $\text{SO}_3$  molecules. In this new chemical mechanism, a loop structure is identified to play a key role in promoting the water-mediated proton transfer that leads to the formation of  $\text{NH}_4\text{HSO}_4$ . Observation of the near-barrierless formation of ammonium bisulfate ( $\text{NH}_4\text{HSO}_4$ ) in the water trimer as well as on surface of a water droplet suggests an alternative dominant channel toward the formation of ammonium sulfate, a major component of aerosol particles in the water droplets.

Born–Oppenheimer AIMD simulation is performed on the basis of density functional theory (DFT) methods as implemented in the CP2K code.<sup>29</sup> The exchange and correlation interactions of electrons are treated with the Becke–Lee–Yang–Parr (BLYP) functional,<sup>30,31</sup> and the Grimme’s dispersion correction method is applied to account for the weak dispersion interaction.<sup>32</sup> A double- $\zeta$  Gaussian basis set combined with an auxiliary basis set<sup>33</sup> and the Goedecker–Teter–Hutter (GTH) norm-conserved

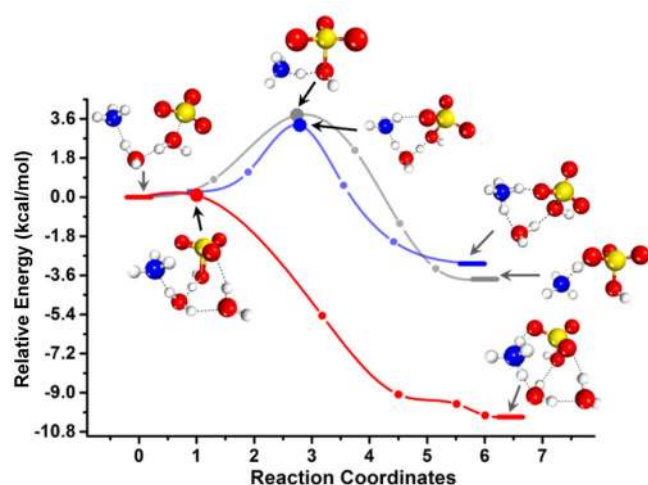


**Figure 1.** A schematic illustration of the energy profiles for the reaction of  $\text{NH}_3$  and  $\text{SO}_3$  molecules with a water monomer (in gray), water dimer (in blue), and water trimer (in red). The horizontal bar denotes the reactant or the product state. The larger solid circles represent the transition states and the smaller solid circles correspond to the replicas in the CI-NEB methods. The white, blue, red and yellow spheres represent H, N, O and S atoms, respectively.

pseudopotentials<sup>34,35</sup> are adopted to treat the valence electrons and the core electrons, respectively. An energy cutoff of 280 Ry is set for the plane wave basis set and 40 Ry for the Gaussian basis set. A supercell ( $20 \times 20 \times 20 \text{ \AA}^3$ ) with periodic boundary conditions is selected for the  $(\text{NH}_3)(\text{SO}_3)(\text{H}_2\text{O})_n$  ( $n = 1-3$ ) systems, which is large enough to neglect interaction between the neighboring replica. For the water droplet system, a relative large supercell with size ( $35 \times 35 \times 35 \text{ \AA}^3$ ) is used. The water droplet with 192 water molecules is carved out from the supercell of pre-equilibrated bulk water at 300 K and re-equilibrated at 300 K for  $\sim 6$  ps. Upon the adsorption of a  $\text{NH}_3$  and a  $\text{SO}_3$  molecule onto the surface of the water droplet, the structure is further optimized at DFT level of theory before the AIMD simulations. All the AIMD simulations are performed in the constant volume and temperature ensemble with the temperature controlled at 300 K. The climbing image nudged-elastic-band (CI-NEB) method is used to locate the transition state.<sup>36,37</sup> In addition, the geometries of reactant and product states are also optimized at the MP2/6-311++G(d,p) level of theory, while the transition state is further confirmed via frequency analysis at the MP2 level of theory, using the Gaussian 09 software. These separated MP2 computations allow confirmation of the activation energy barrier for each reaction.

First, we compute the energy barrier to the formation of  $\text{NH}_4\text{HSO}_4$  from  $\text{NH}_3$  and  $\text{SO}_3$  associated with one or two water molecules, using the CI-NEB method. For the water monomer system, as shown in Figure 1, the splitting of the water molecule requires to overcome an energy barrier of  $\sim 3.78$  kcal/mol (3.96 kcal/mol at the MP2/6-311++G(d,p) level), consistent with a previous study.<sup>22</sup> Upon splitting of the water molecule, both  $\text{OH}^-$  ion and the proton bind with the  $\text{SO}_3$  molecule, leading to the exclusive formation of  $\text{H}_2\text{SO}_4$ . In contrast, the inclusion of an extra water molecule in the dimer system can promote the proton transfer from the water molecule to the  $\text{NH}_3$  molecule and stabilize the  $\text{NH}_4^+$  due to the added hydration effect. As shown in Figure 1, the proton of one water molecule that is near the  $\text{SO}_3$  shifts toward the other water molecule that interacts directly with  $\text{NH}_3$ . Meanwhile, the proton of the other water molecule shifts toward

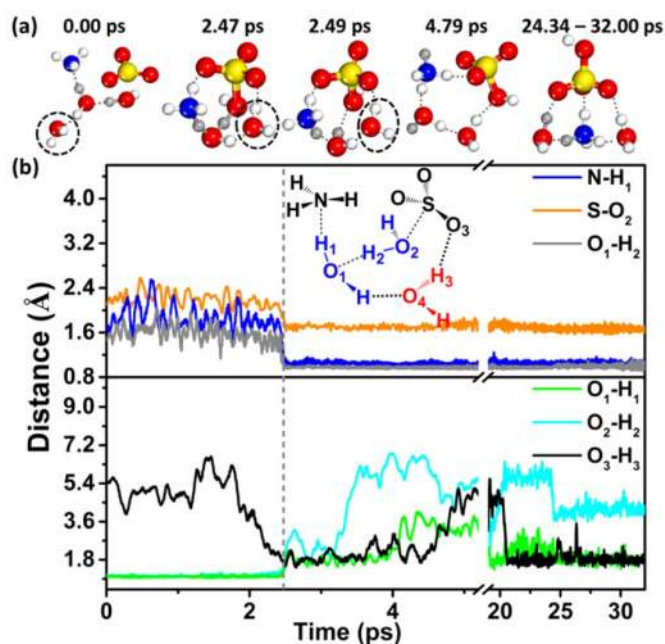


**Figure 2.** (a) Snapshot structures taken from the AIMD simulation of the water trimer system with the  $\text{NH}_3$  and  $\text{SO}_3$  molecules. The gray spheres mark the transferred protons during the reaction. (b) The time evolution of the N-H<sub>1</sub>, S-O<sub>2</sub>, O<sub>1</sub>-H<sub>2</sub>, O<sub>1</sub>-H<sub>1</sub>, O<sub>2</sub>-H<sub>2</sub>, and O<sub>3</sub>-H<sub>3</sub> lengths in the course of the AIMD simulation. The inset illustrates the loop structure formed prior to the formation of the  $\text{NH}_4^+/\text{HSO}_4^-$  ion pair.

$\text{NH}_3$ , leading to the formation of  $\text{NH}_4^+$ , while the remaining  $\text{OH}^-$  ion binds with the  $\text{SO}_3$  to form  $\text{HSO}_4^-$ . Overall the water molecule near  $\text{NH}_3$  acts as a proton transporter by accepting the proton from one source and delivering it to another molecule. Such a reaction mechanism can be viewed as a water-mediated proton-transfer mechanism as previously reported,<sup>38</sup> and this mechanism enables the formation of  $\text{NH}_4^+/\text{HSO}_4^-$  ion pair in the dimer system with a slightly lower barrier of  $\sim 3.30$  kcal/mol (3.80 kcal/mol at the MP2/6-311++G(d,p) level). However, during the AIMD simulations of both water monomer and dimer systems, neither the  $\text{NH}_4^+/\text{HSO}_4^-$  ion pair nor  $\text{NH}_3/\text{H}_2\text{SO}_3$  complex is observed due largely to the notable energy barriers for the formation reactions (see Figures S1 and S2, and Movies S1 and S2).

In the atmosphere, although the population of the water trimers is about 1 order of magnitude less than that of the water dimers,<sup>39,40</sup> the water trimer may still play a key role in certain chemical reactions if the hydration effect becomes increasingly important with increasing the size of water clusters. This is indeed the case for the formation of ammonium bisulfate. Unlike the water monomer and dimer systems, the formation of  $\text{NH}_4\text{HSO}_4$  can be directly observed during the AIMD simulation with the water trimer system (Movie S3). As shown in Figure 2a, the  $\text{SO}_3$  molecule is fully hydrated by the water trimer (set as the initial configuration) through the donor-acceptor interaction between the  $\pi$  orbital of  $\text{SO}_3$  and the p orbital of atomic O, while the  $\text{NH}_3$  molecule only interacts with the water molecule via the N-H<sub>1</sub> hydrogen bond (H-bond). Initially ( $< 2.47$  ps) the N-H<sub>1</sub> and S-O<sub>2</sub> lengths only fluctuate around 1.80 and 2.10 Å, respectively, without showing any bond formation. At  $\sim 2.47$  ps, a shift of the dangling water molecule (the circled molecule in Figure 2a) toward the  $\text{SO}_3$  molecule shortens the O<sub>3</sub>-H<sub>3</sub> length to  $\sim 1.60$  Å and reduces the  $\text{H}_3\text{O}_4\text{O}_3$  angle to  $< 30^\circ$  (see black line in Figure 2b and Figure S3), leading to the formation of an



H-bond between the dangling water molecule and the  $\text{SO}_3$ . This leads to a loop structure involving the water trimer and  $\text{SO}_3$ , as shown in the snapshot at 2.47 ps (see also the inset in Figure 2b). Upon the formation of the loop structure, the  $\text{O}_1\text{--H}_1$  and  $\text{O}_2\text{--H}_2$  lengths are elongated to  $\sim 1.75$  and  $2.09$  Å, respectively, suggesting the breakage of O–H bonds. On the other hand, the  $\text{N--H}_1$  and  $\text{O}_1\text{--H}_2$  lengths decrease to  $\sim 1.04$  and  $0.96$  Å, respectively, suggesting the formation of new N–H and O–H bonds. This bond length evolution involves transfer of two protons, resulting in the formation of  $\text{NH}_4^+$  and regeneration of a water molecule (Figure 2a). Meanwhile, the remaining  $\text{OH}_2$  group quickly binds with  $\text{SO}_3$ , giving rise to  $\text{HSO}_4^-$ . After the  $\text{NH}_4^+/\text{HSO}_4^-$  ion pair is formed with two water molecules (Movie S3), no significant change in the  $\text{N--H}_1$  and the  $\text{S--O}_2$  bonds is seen, suggesting the unlikelihood of the reverse reaction. Note that the water trimer we considered here entails a linear structure. The formation of the  $\text{NH}_4^+/\text{HSO}_4^-$  ion pair is also observed in an independent AIMD simulation with a loop-shaped water trimer as the initial structure. With the latter, the reaction proceeds even faster (Movie S4). The direct observation of the formation of the  $\text{NH}_4^+/\text{HSO}_4^-$  ion pair with the water trimer indicates the reaction is nearly barrierless. This is also confirmed from our independent reaction path computation using the CI-NEB method (see Figure 1). The computed energy barrier is merely  $\sim 0.08$  kcal/mol (less than the factor  $k_B T$ , where the temperature  $T = 300$  K and  $k_B$  is the Boltzmann constant).

Overall, the formation mechanism of the  $\text{NH}_4^+/\text{HSO}_4^-$  ion pair in the water trimer system is quite similar to that for the dimer system, but involves a very low barrier. As shown in the inset of Figure 2b, the two water molecules (in blue) act as the reaction center where the water molecule having  $\text{O}_1$  plays the role of proton transporter, i.e., to accept and deliver the proton. The extremely low barrier is largely due to the formation of a loop structure involving the third water molecule. Moreover, the presence of the third water molecule results in a stronger exothermic reaction ( $\sim 10.12$  kcal/mol), thereby further enhancing the stability of  $\text{NH}_4\text{HSO}_4$ . We have also simulated the reaction of  $\text{NH}_3$  and  $\text{SO}_3$  in a water tetramer system. As shown in Figure S4, no reaction barrier is seen during the formation of  $\text{NH}_4^+/\text{HSO}_4^-$  ion pair, while the same reaction mechanism is observed as in the trimer system. In the AIMD simulation, the proton transfer occurs at  $\sim 0.44$  ps (Movie S5), suggesting relatively faster formation of  $\text{NH}_4^+/\text{HSO}_4^-$  ion pair.

Previous studies suggest that water droplets in the upper troposphere ( $> 2$  km) may play an important role in the atmospheric chemistry.<sup>41–44</sup> Particularly, the water–air interface has been suggested as the key area for many important chemical processes,<sup>45–47</sup> such as the ionization of  $\text{N}_2\text{O}_4$ ,<sup>48</sup> the acid formation from sulfur, nitrogen oxide and organic compounds,<sup>49</sup> and the  $\text{Cl}_2$  formation from the  $\text{Cl}^-$  oxidation,<sup>50</sup> among others. We have performed an independent AIMD simulation of the formation of the  $\text{NH}_4^+/\text{HSO}_4^-$  ion pair on the surface of a water droplet upon the adsorption of a  $\text{NH}_3$  and a  $\text{SO}_3$ . A loop-structure promoted proton-transfer mechanism is observed as in the water trimer and tetramer systems. As shown in the Figure S5, prior to the reaction, the  $\text{N--S}$  bond length varies from  $\sim 4.00$  to  $11.00$  Å, indicating no direct interaction between  $\text{NH}_3$  and  $\text{SO}_3$ . Figure 3a,  $\text{SO}_3$  forms a cyclic structure with four water molecules at  $\sim 4.96$  ps. Notably, such a cyclic structure differs from the loop structure obtained in the water trimer system. As shown in Figure 3b, the  $\text{O}_2\text{--H}_2$  length is shortened to  $\sim 2.10$  Å (marked by the gray arrow), whereas the  $\text{O}_2\text{--H}_4$  length still maintains to be  $\sim 2.10$  Å, indicating the formation of two H-bonds with a single oxygen

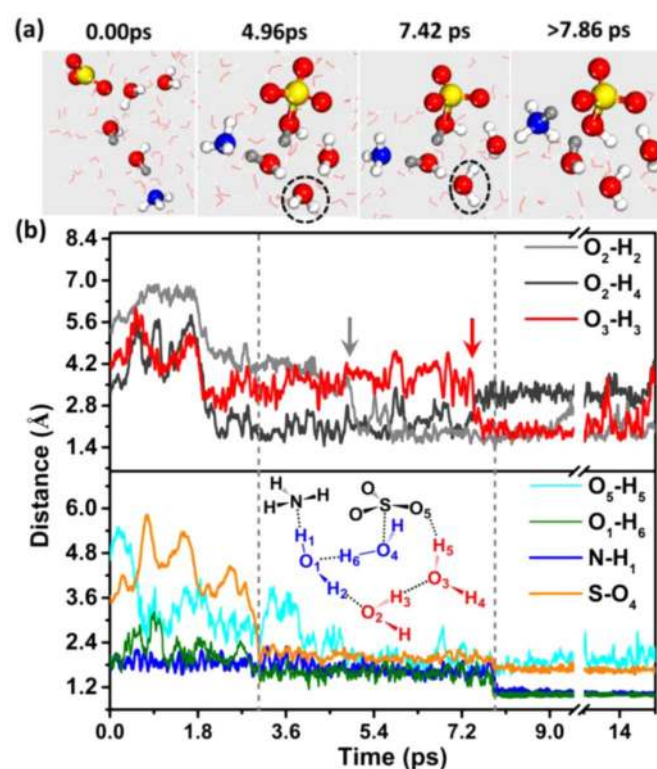


**Figure 3.** (a) Snapshot structures taken from the AIMD simulation of the  $\text{NH}_3$  and  $\text{SO}_3$  molecules adsorbed on the surface of a water nanodroplet. The gray spheres mark the transferred protons during the reaction. (b) The time evolution of the  $\text{O}_2\text{--H}_2$ ,  $\text{O}_2\text{--H}_4$ ,  $\text{O}_3\text{--H}_3$ ,  $\text{O}_5\text{--H}_5$ ,  $\text{O}_1\text{--H}_6$ ,  $\text{N--H}_1$ , and  $\text{S--O}_4$  lengths (see the inset for definition of atom–atom lengths) in the course of the AIMD simulation. The inset illustrates the loop structure formed prior to the formation of the  $\text{NH}_4^+/\text{HSO}_4^-$  ion pair.

atom not seen in the loop structure. Beyond 7.42 ps (marked by the red arrow), the  $\text{O}_2\text{--H}_4$  length increases to  $\sim 3.20$  Å, accompanied by the decrease of the  $\text{O}_3\text{--H}_3$  length from 3.50 to  $\sim 2.10$  Å due to the flipping over of the circled water molecule shown in Figure 3a. The flip transforms the cyclic structure into a loop structure, as observed in the water trimer system where only one H-bond is formed with each oxygen atom. Such behavior is also suggested based on the analysis of the orientation variation of water molecules (Figure S6). Again, the formation of the loop structure stimulates the proton transfer among the water and  $\text{NH}_3$  molecules and results in the breaking of the  $\text{O}_1\text{--H}_1$  and the  $\text{O}_4\text{--H}_6$  bonds (Figure S5) and the formation of the  $\text{O}_1\text{--H}_6$  bond (Figure 3b and Movie S6). Concurrently, the  $\text{N--H}_1$  and the  $\text{S--O}_4$  lengths are shortened to  $\sim 1.07$  and  $1.68$  Å, respectively, indicating the formation of the  $\text{NH}_4^+$  and ions. Also, as shown in the inset of Figure 3b, the proton-transfer mediated by the water molecule occurs in the reaction center, which involves a water dimer (in blue) and a  $\text{NH}_3$  molecule. The other two water molecules (in red) act as the “bridge” to form the loop structure. Hence, both the water trimer and the water-droplet systems demonstrate the same mechanism for the formation of the  $\text{NH}_4^+/\text{HSO}_4^-$  ion pair.

In conclusion, we have provided direct AIMD simulation evidence for the formation of  $\text{NH}_4\text{HSO}_4$  from the separately hydrated  $\text{NH}_3$  and  $\text{SO}_3$  molecules in a water trimer and on the surface of a water droplet. In both systems, direct interaction (adduct) of  $\text{NH}_3$  and  $\text{SO}_3$  is not observed, whereas the  $\text{NH}_4^+/\text{HSO}_4^-$  ion pair is formed instead, following a loop-promoted proton-transfer mechanism. In this mechanism, two water

molecules that directly interact with  $\text{NH}_3$  and  $\text{SO}_3$  serve as the reaction center, while the third water molecule acts as a “bridge” to connect the reaction center with the  $\text{SO}_3$  molecule to form a loop structure. The proton transfer in the reaction center is akin to that in the dimer system where one water molecule acts as a proton transporter. Our computations show that the loop structure formed in the water trimer and water-droplet systems can greatly promote the proton transfer in the reaction center, leading to a near-barrierless reaction. The AIMD simulation provides atomic-level mechanistic insight into the formation of ammonium bisulfate that can be a major precursor for the formation of ammonium sulfate. The latter is known to be a major component in the liquid droplet of aerosols, e.g., the  $\text{PM}_{2.5}$  microparticles.

### Supporting Information

Time evolution of the interatomic distances for the monomer, the dimer and the water-droplet systems; angular variation of water molecules in the water trimer and the water-droplet systems; the schematic illustration of the energy profiles for the reaction of  $\text{NH}_3$  and  $\text{SO}_3$  in the water tetramer systems; coordinates of the transition states for the water monomer, dimer and trimer systems; movies of trajectories of the AIMD simulations for the monomer, the dimer, the trimer, the tetramer and the water-droplet systems.

The Supporting Information is attached to the repository record for this article; it is also available free of charge on the ACS Publications website at DOI: 10.1021/jacs.5b13048.

**Acknowledgments** — We thank Professor Jun Wang for valuable discussions. This work is supported by the National Science Foundation (CHE- 1500217), USTC Qin-ren B (1000-Talents Program B) fund for Summer Research, and by the University of Nebraska Holland Computing Center. The authors declare no competing financial interest.

### References

- (1) Chameides, W. L.; Yu, H.; Liu, S. C.; Bergin, M.; Zhou, X.; Mearns, L.; Wang, G.; Kiang, C. S.; Saylor, R. D.; Luo, C.; Huang, Y.; Steiner, A.; Giorgi, F. *Proc. Natl. Acad. Sci. U. S. A.* 1999, 96, 13626.
- (2) Breon, F. M.; Tanre, D.; Generoso, S. *Science* 2002, 295, 834.
- (3) Charlson, R. J.; Schwartz, S. E.; Hales, J. M.; Cess, R. D.; Coakley, J. A.; Hansen, J. E.; Hofmann, D. J. *Science* 1992, 255, 423.
- (4) Menon, S.; Hansen, J.; Nazarenko, L.; Luo, Y. F. *Science* 2002, 297, 2250.
- (5) Ramanathan, V.; Crutzen, P. J.; Kiehl, J. T.; Rosenfeld, D. *Science* 2001, 294, 2119.
- (6) Tegen, I.; Lacis, A. A.; Fung, I. *Nature* 1996, 380, 419.
- (7) Kim, K. H.; Kabir, E.; Kabir, S. *Environ. Int.* 2015, 74, 136.
- (8) Davidson, C. I.; Phalen, R. F.; Solomon, P. A. *Aerosol Sci. Technol.* 2005, 39, 737.
- (9) Kiehl, J. T.; Briegleb, B. P. *Science* 1993, 260, 311.
- (10) Abbatt, J. P. D.; Benz, S.; Cziczo, D. J.; Kanji, Z.; Lohmann, U.; Mohler, O. *Science* 2006, 313, 1770.
- (11) Poschl, U. *Angew. Chem., Int. Ed.* 2005, 44, 7520.
- (12) Sun, Y. L.; Du, W.; Wan, Q. Q.; Zhang, Q.; Chen, C.; Chen, Y.; Chen, Z. Y.; Fu, P. Q.; Wang, Z. F.; Gao, Z. Q.; Worsnop, D. R. *Environ. Sci. Technol.* 2015, 49, 11340.
- (13) Kulmala, M.; Petaja, T.; Ehn, M.; Thornton, J.; Sipila, M.; Worsnop, D. R.; Kerminen, V. M. *Annu. Rev. Phys. Chem.* 2014, 65, 21.
- (14) Hua, W.; Verreault, D.; Allen, H. C. *J. Am. Chem. Soc.* 2015, 137, 13920.
- (15) Coffman, D. J.; Hegg, D. A. *J. Geophys. Res.* 1995, 100, 7147.
- (16) Hofmann, M.; Schleyer, P. V. J. *J. Am. Chem. Soc.* 1994, 116, 4947.
- (17) Morokuma, K.; Muguruma, C. *J. Am. Chem. Soc.* 1994, 116, 10316.
- (18) Steudel, R. *Angew. Chem., Int. Ed. Engl.* 1995, 34, 1313.
- (19) Gonzalez, J.; Torrent-Sucarrat, M.; Anglada, J. M. *Phys. Chem. Chem. Phys.* 2010, 12, 2116.
- (20) Hazra, M. K.; Sinha, A. J. *J. Am. Chem. Soc.* 2011, 133, 17444.
- (21) Vandenheuvel, A. P.; Mason, B. J. Q. *J. R. Meteorol. Soc.* 1963, 89, 271.
- (22) Larson, L. J.; Tao, F. M. *J. Phys. Chem. A* 2001, 105, 4344.
- (23) Renard, J. J.; Calidonna, S. E.; Henley, M. V. *J. Hazard. Mater.* 2004, 108, 29.
- (24) Canagaratna, M.; Phillips, J. A.; Goodfriend, H.; Leopold, K. R. *J. Am. Chem. Soc.* 1996, 118, 5290.
- (25) Hunt, S. W.; Brauer, C. S.; Craddock, M. B.; Higgins, K. J.; Nienow, A. M.; Leopold, K. R. *Chem. Phys.* 2004, 305, 155.
- (26) Lovejoy, E. R.; Hanson, D. R. *J. Phys. Chem.* 1996, 100, 4459.
- (27) Pawlowski, P. M.; Okimoto, S. R.; Tao, F. M. *J. Phys. Chem. A* 2003, 107, 5327.
- (28) Shi, Z.; Ford, J. V.; Castleman, A. W. *Chem. Phys. Lett.* 1994, 220, 274.
- (29) VandeVondele, J.; Krack, M.; Mohamed, F.; Parrinello, M.; Chassaing, T.; Hutter, J. *Comput. Phys. Commun.* 2005, 167, 103.
- (30) Becke, A. D. *Phys. Rev. A: At., Mol., Opt. Phys.* 1988, 38, 3098.
- (31) Lee, C. T.; Yang, W. T.; Parr, R. G. *Phys. Rev. B: Condens. Matter Mater. Phys.* 1988, 37, 785.
- (32) Grimme, S.; Antony, J.; Ehrlich, S.; Krieg, H. *J. Chem. Phys.* 2010, 132, 154104.
- (33) VandeVondele, J.; Hutter, J. *J. Chem. Phys.* 2007, 127, 114105.
- (34) Hartwigsen, C.; Goedecker, S.; Hutter, J. *Phys. Rev. B: Condens. Matter Mater. Phys.* 1998, 58, 3641.
- (35) Goedecker, S.; Teter, M.; Hutter, J. *Phys. Rev. B: Condens. Matter Mater. Phys.* 1996, 54, 1703.
- (36) Mills, G.; Jonsson, H.; Schenter, G. K. *Surf. Sci.* 1995, 324, 305.
- (37) Henkelman, G.; Uberuaga, B. P.; Jonsson, H. *J. Chem. Phys.* 2000, 113, 9901.
- (38) Loerting, T.; Liedl, K. R. *J. Phys. Chem. A* 2001, 105, 5137.
- (39) Anglada, J. M.; Hoffman, G. J.; Slipchenko, L. V.; Costa, M. M.; Ruiz-Lopez, M. F.; Francisco, J. S. *J. Phys. Chem. A* 2013, 117, 10381.
- (40) Gonzalez, J.; Caballero, M.; Aguilar-Mogas, A.; Torrent-Sucarrat, M.; Crehuet, R.; Sole, A.; Gimenez, X.; Olivella, S.; Bofill, J. M.; Anglada, J. M. *Theor. Chem. Acc.* 2011, 128, 579.
- (41) Heicklen, J. *Atmos. Environ.* 1981, 15, 781.
- (42) Napari, I.; Makkonen, R.; Kulmala, M.; Vehkamäki, H. *Atmos. Res.* 2006, 82, 514.
- (43) Zhao, Y.; Li, H.; Zeng, X. C. *J. Am. Chem. Soc.* 2013, 135, 15549.
- (44) Zhong, J.; Zhao, Y.; Li, L.; Li, H.; Francisco, J. S.; Zeng, X. C. *J. Am. Chem. Soc.* 2015, 137, 12070.
- (45) Tobias, D. J.; Stern, A. C.; Baer, M. D.; Levin, Y.; Mundy, C. J. *Annu. Rev. Phys. Chem.* 2013, 64, 339.
- (46) Clifford, D.; Donaldson, D. J. *J. Phys. Chem. A* 2007, 111, 9809.
- (47) Gerber, R. B.; Varner, M. E.; Hammerich, A. D.; Riikonen, S.; Murchaew, G.; Shemesh, D.; Finlayson-Pitts, B. J. *Acc. Chem. Res.* 2015, 48, 399.
- (48) Miller, Y.; Finlayson-Pitts, B. J.; Gerber, R. B. *J. Am. Chem. Soc.* 2009, 131, 12180.
- (49) Calvert, J. G.; Lazrus, A.; Kok, G. L.; Heikes, B. G.; Walega, J. G.; Lind, J.; Cantrell, C. A. *Nature* 1985, 317, 27.
- (50) Knipping, E. M.; Dabdub, D. *Environ. Sci. Technol.* 2003, 37, 275.